# Photoelectrochemical water splitting by triazine based covalent organic framework

Bidhan Chandra Patra,[†] SantimoyKhilari,[§] Mathew Adicoat,[¶] DebabrataPradhan,[§] AnirbanPradhan,*[,†] Santanu Bhattacharya*[,†]

[†]*Director's Research Unit, Indian Association for the Cultivation of Science, Jadavpur, Kolkata-700032, INDIA.*
[§]*Indian institute of Technology Kharagpur, Kharagpur-721302, INDIA.*
[¶]*School of Science and Technology, Nottingham Trent University, Clifton Lane, Nottingham, NG11 8NS, UK.*

KEYWORDS: Photoelectrochemical water splitting, hydrogen evolution, DFT calculation, band gap.

**ABSTRACT:** Photo electrochemical (PEC) water splitting under visible light irradiation is a very promising path for green and sustainable hydrogen production. PEC process has gained enormous research interested due to the potential of direct conversion of solar power into chemical fuel. Herein, we developed a covalent organic framework (COFs) which promise as an ideal photoabsorber due to the combination of efficient light harvesting sites with suitable band gap and catalytic sites for HER. Under solvothermal condition a Schiff base type condensation between 1,3,5-tris (4-formylbiphenyl) benzene (TFBB), 2, 4, 6-Tris(4-aminophenyl)-1, 3, 5-triazine (TAT) and 2, 4, 6-Tris(4-aminophenyl)-benzene (TAB) yields a crystalline, 2-D covalent organic frameworks TFBB-TAT and TFBB-TAB COF respectively. The as prepared triazine containing TFBB-TAT COF shows better photo electrochemical (PEC) water splitting compare to non triazine based TFBB-TAB COF. This work enriches the structural variety of COFs plays an important role on PEC water splitting but also provides an intriguing electrochemical behaviour of these class.

## INTRODUCTION:

Progressive decrease of fossil fuel preservers causes an acute urgency for clean, sustainable and environmentally viable energy sources.[1,2] Till now, solar energy is the highest sustainable energy source towards the global energy supply. During the last decades, several research groups around the world continuously try to improve and develop most viable excellent visible light photocatalytic system as a green technology which is capable of direct conversion of solar energy into energy, store in the bonds of "solar fuels" or "chemical fuels" such as hydrogen.[3-5] However, the biggest challenges for large scale utilization of these green technologies are minimizing the hydrogen production cost with maximising the efficiency at a lower economic investment. This problem can be solved by using photo electrochemical (PEC) water splitting cells which directly split water in presence of sunlight to hydrogen and oxygen at cathode and anode respecively.[6-8] Thus development of efficient photocatalytic system became an active field of energy research to design efficient photoelectrodes. For this purpose, the physicochemical properties of PEC catalyst such as suitable band gap, favourable band edge positions, surface area, morphology, interfacial charge transfer kinetics and corrosion stability plays important role.[9-11] Various inorganic and organic photocatalyst has been developed but compare to inorganic semiconductors, organic semiconductors such as graphitic carbon nitride (g-$C_3N_4$) and its modifiers have been widely exploited due to their tailored structure, excellent electronic properties and diverse synthetic modularity.[12-16]

Covalent organic framework (COF) is a class of crystalline porous material in which organic monomers integrate to form a periodic framework.[17-20] Last few years COFs have been evolved as a new photoactive materials for light-induced hydrogen evolution because of the high electron density with extended π-stacked structure similar to g-$C_3N_4$ as well as distinct porosity.[21] Further, the photochemical activity will be well synchronized by the selection of proper building unit. COFs are modular, versatile, and adaptive as they are characterized by an easy tunability of (opto) electronic properties, structure, crystallinity, and porosity. They are mainly composed of highly abundant organic elements (C, H, N, O, S *etc*.) which will incorporate synthetic versatility for construction of heterogeneous photocatalysis. The extended in plane π-electron conjugation together with the possibility of axial charge transport in the stacking direction by the overlap of π-orbitals can result in high charge carrier mobility.[22-23] Such characteristics of supramolecular COFs architectures promotes light harvesting and charge transport capacity.

Photoelectrochemical water splitting is mainly determined by two key factors. One is the suitable valance and conduction band position in which the electrons are exited from valence band by photon irradiation. Mostly, the photoactive characteristics of nitrogen reach COF is determined by the nitrogen group present in the COF system. In this context the triazine moiety was found to be a promising photo absorber site in various polymer or COF systems. The band position of triazine containing photocatalystsis mostly influenced by the $N_{2p}$ orbitals of triazine moiety. The second PEC governing factor is the electrocatalytic activation of proton by charge recombination to generate molecular hydrogen. Upto now, the modified g-$C_3N_4$ and its derivatives were used as a stable photocatalyst for proton reduction under visible light irradiation. However, their improper band alignment retards the efficiency for proton reduction. Recently, Jijia et al reported a covalent triazine polymer/COF by changing the C and N ratio, making the suitable band alignment for proton reduction as well

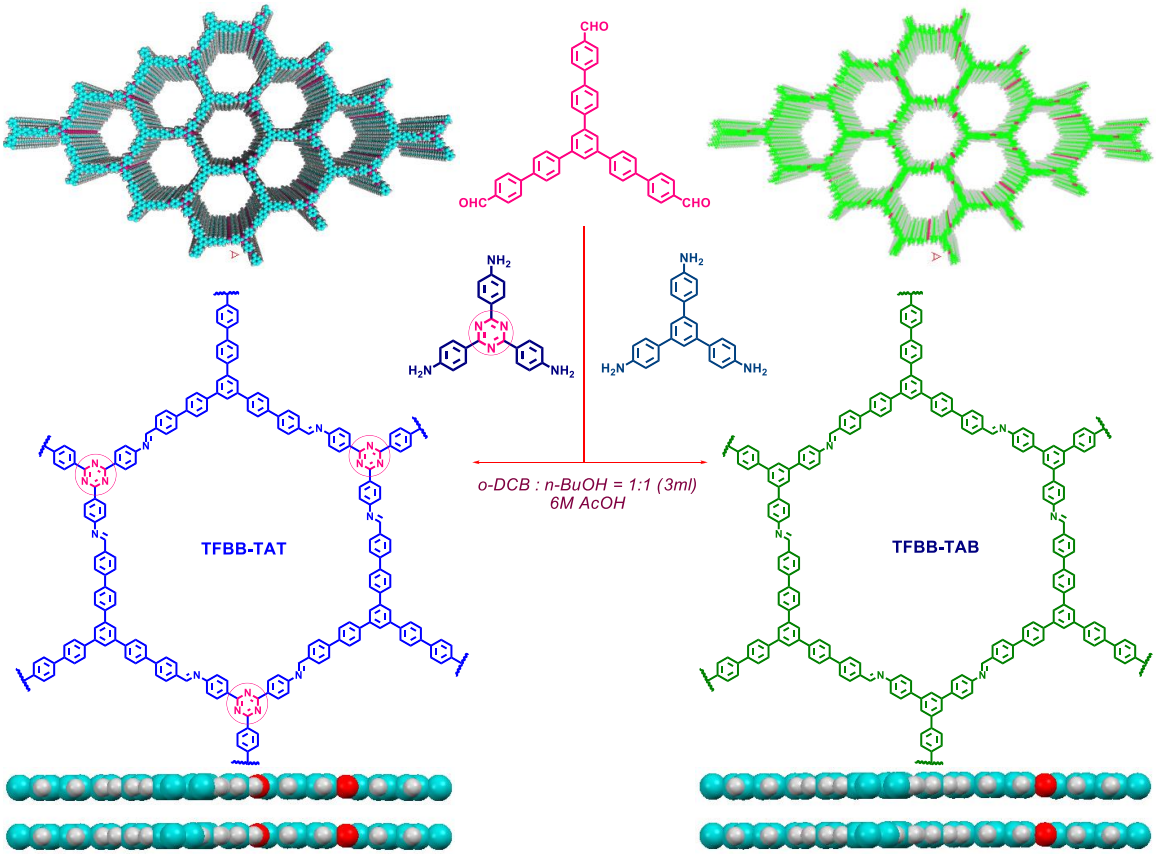


**Scheme 1:** Schematic presentation of TFBB-TAT and TFBB-TAB COF

as water oxidation.[24] A very few imine and hydrazone-based COFs have been explored for photo electrochemical (PEC) water splitting under visible light irradiation.[25] There is some significant drawback for such kind of COFs materials due to their instability and poor energy conversion in neutral water. In our previous study, we reported porphyrin based metal free COP/COF for electrochemical water splitting in acidic medium.[26-27] Last few years Lotsch *et al* explored covalent triazine-based COFs materials as a photocatalyst which have high thermal and chemical stability.[28-29] The extended π-staking in triazine based COFs promotes exciton separation and excellent charge transport properties which is highly preferred for photocatalysis.[30,] So far, they have been explored as potential sorbents and catalytic support.[31] The extended exploration and comparison with triazine-based COFs and similar COFs structure without central triazine was not explored yet for photocatalysis. Based upon these superior performance of the triazine functional covalent triazine framework (CTF), herein we introduce a triazine based covalent organic framework (TFBB-TAT) which shows the favourable water splitting compare with the triazine free counterpart TFBB-TAB COF (**Scheme 1**). The diversity and easily tailored structures for tunable water splitting capacity may not only widen the scope of organic semiconductor but also provide a molecular level understanding and comparison of the inherent heterogeneous photocatalysis.

## RESULTS AND DISCUSSION:

The crystallinity of both TFBB-TAT and TFBB-TABCOFS were assessed by the powder x-ray diffraction (PXRD) analysis (**figure 1**a & c). An intense peak at 2θ value of 3.27° and 3.16° was observed for TFBB-TAT and TFBB-TAB COF, indicates the first (100) plane. Other minor peaks ~ 5.4° and 6.2° indicate the presence of (210) and (200) planes respectively. The broad peak for TFBB-TAT COF observed at ~25° (2θ) stipulates the (001) plane, which indicates the presence of strong interlayer stacking. This large stacking is due to the planner triazine unit (coming from TAT) in the COF crystallites, which is absent for the TFBB-TAB COF. Due to the presence of non-planner central phenyl ring (coming from TAB), interlayer stacking for TFBB-TAB COF is very poor. Pawley refinement was carried out to define exact lattice packing for both of these COFs in which TFBB-TAT shows slip-AA mode with stacking energy -286.3 kcal mole$^{-1}$ and TFBB-TAB COF also shows slip-AA stacking with -284.62 kcal mole$^{-1}$ stabilization energy. Moreover, the experimental PXRD pattern also matches well with these stacking modes. After refinement, the unit cell parameter was calculated to be $a$ = 33.21 Å, $b$ = 34.33, $c$ = 6.94 Å, α = β = 90°, γ = 59° ($R_{wp}$ = 5.38%, $R_p$ = 3.27%) for TFBB-TAT COF and $a$ = 33.44 Å, $b$ = 34.51, $c$ = 6.46 Å, α = β = 90°, γ = 59° ($R_{wp}$ = 3.48%, $R_p$ = 2.48%) for TFBB-TAB COF (**figure 1**b & d). Stabilization of this slipped-AA stacking over the eclipsed (AA) stacking is due to less repulsion between the atoms where the atom lies slightly offset to the adjacent layers. To pledge the permanent porosity of these two COFs (TFBB-TAT and TFBB-TAB), $N_2$ adsorption-desorption measurement were carried out. From the isotherm plot, it is clear that there is a typical type IV adsorption isotherm with surface area 430 m$^2$ g$^{-1}$ and 130 m$^2$ g$^{-1}$ for TFBB-TAT(**figure 2**a) and TFBB-TAB COF (**figure 2**b) respectively. The surface area were calculated by taking the value of relative pressure ($P/P_0$) from 0.07 to 0.2 with a total pore volume of 0.244 cc g$^{-1}$ and 0.05 cc g$^{-1}$ for TFBB-TAT and TFBB-TAB respectively at $P/P_0$ = 0.99.

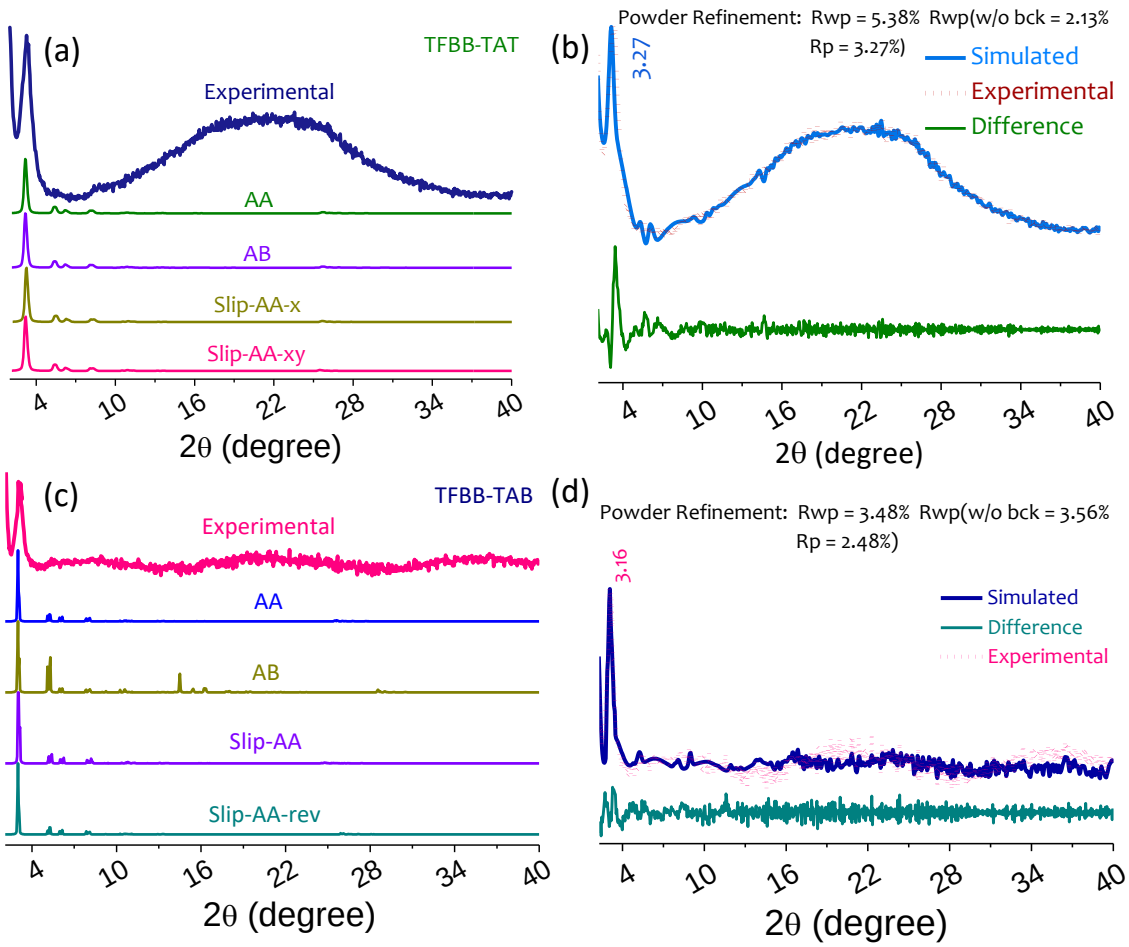


**Figure 1**: (a, c) Experimental and theoretical powder x-ray diffraction comparison of TFBB-TAT and TFBB-TAB COF respectively. (b, d) Powley refinement of the experimental PXRD of TFBB-TAT and TFBB-TAB COF respectively.

High surface area for TFBB-TAT was measured, due to the strong stacking throughout long channels of COF crystallite. It is reported that the central triazine moiety is more planar than the central phenyl ring with respect to the other phenyl ring in both the COFs.[ref] This make the TFBB-TAT COF more planar, causes large interlayer stacking.Different carbon environment was confirmed by the solid state $^{13}C$ cross polarisation magic angle spinning (CP-MAS) NMR spectroscopy. Characteristic imine bonded carbon (-C=N-) was reaffirmed by the chemical shift of ~164 ppm for TFBB-TAT and ~162 ppm for TFBB-TAB. One extra deshielded peak at 173 ppm, was confirmed the presence of triazine carbon atom of TFBB-TAT COF, which is absent in the TFBB-TAB COF (**figure 2**k).Fourier transformer infrared spectroscopy (FT-IR) unveil the presence of aldehyde -C-H stretching band of TFS at 2730 $cm^{-1}$ which is impaired after the condensation reaction to form TFBB-TAT and TFBB-TAB COF (**Figure 2**l). This indicates full depletion of the starting aldehyde. Total consumption of starting amine was also confirmed by the attenuate of –N=H stretching of 3470 $cm^{-1}$ (TAT) and 3433 $cm^{-1}$ (TAB) in both of the COF TFBB-TAT and TFBB-TAB respectively. Imine bond (-C=N-) formation was further confirmed by the appearance of a new peak at 1697 $cm^{-1}$ for both the COFs, which was absent in all the precursors (TFBB, TAT, TAB). Morphological studies were investigated by the transmission electron microscopy (TEM) and scanning electron microscopy (SEM) (**Figure 2** c-j). From the HR-TEM images, it is obvious that both the COFs form the hollow tubular morphology with thickness of ~400 nm, having internal diameter of ~200 nm.

SEM images also support the same morphology aforementioned by the TEM analysis. Presence of elemental carbon and nitrogen was confirmed by the X-ray photoelectron spectroscopy (XPS). The high resolution XPS analysis shows the presence of two types $C_{1s}$ at 283.7 evand 287 eV for TFBB-TAT. This is due the presence of -C=C and -C=N carbon atom in the TFBB-TAT COF moiety. Further, the N 1s XPS peak at ~398.5 eV indicates the presence -C=N functionality in the TFBB-TAT COF.

## PHOTOELECTROCHEMICAL ACTIVITY:

The synthesized COFs were employed as photoelectrocatalysts for water to hydrogen production in PEC. The photocathodes were designed by employing the COF material on the PEDOT: PSS modifies ITO surface. The PEDOT: PSS layer on ITO substrate serves as a hole transporting candidate in the photocathode. Further, the COF layer on the photocathode was in direct contact with the aqueous electrolyte. The cathodic water reduction capacity of the as synthesized COFs in PEC was studied from the polarization plots under dark and illuminated conditions. Figure 3a shows cathodic polarization plots of as synthesized COFs modified photocathodes under dark and illuminated condition. A notable increment of cathodic current density was noticed on switching from dark to illumination condition. This enhancement of cathodic response attributed to the photoreactivity of the as synthesized COFs. The improved negative current density upon illumination was originates from the electron-hole pair generation on the COF surface followed by transfer of the hole to

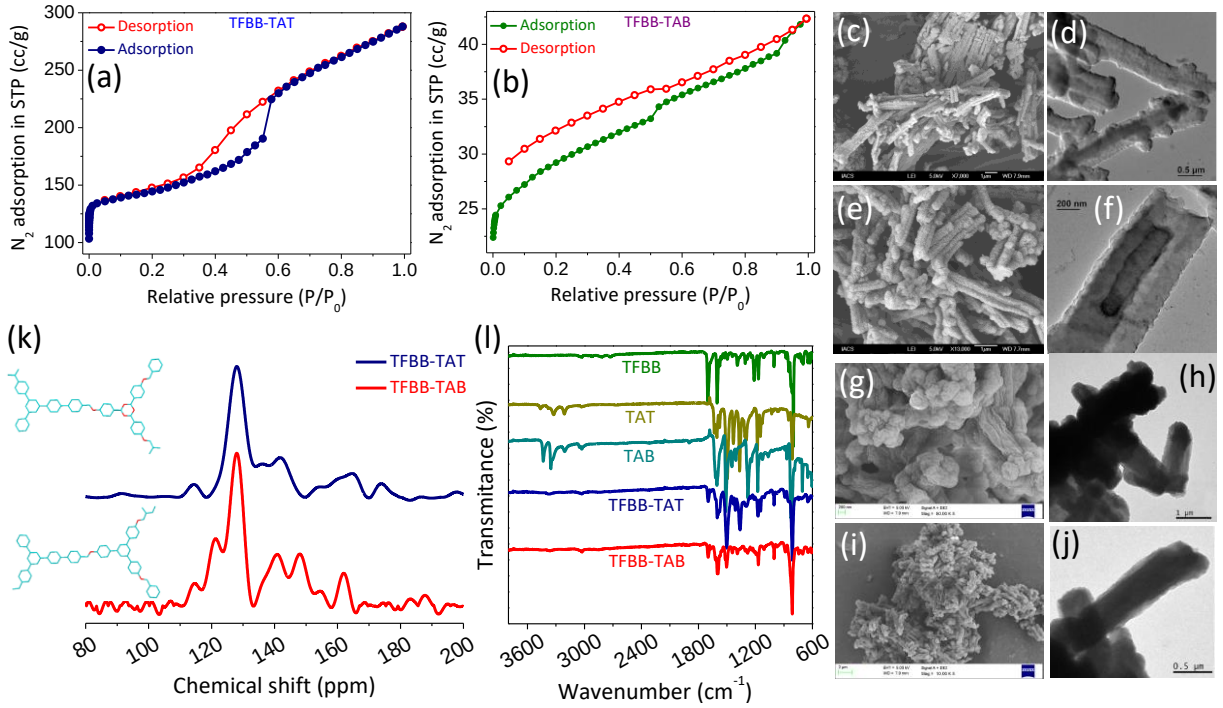


**Figure 2**: (a) $N_2$ adsorption/desorption isotherm of TFBB-TAT and TFBB-TAB COF respectively. (c, e) SEM images of TFBB-TAT COF. (d, f) HR-TEM images of TFBB-TAT COF. (g, i) SEM images of TFBB-TAB COF. (h, j) HR-TEM images of TFBB-TAT COF (k) ss13C MAS NMR spectra of TFBB-TAT and TFBB-TAB COF. (l) FT-IR spectra of TFBB-TAT and TFBB-TAB COF.

PEDOT: PSS/ITO and electrons moves to the electrolyte leading to the water reduction.[32]

The water reduction efficacy of a photocathode is generally determined from the magnitude of current density at 0 V vs. RHE, which signifies thermodynamic bias free condition. In present study, TFBB-TAT containing phtocathode deliver a current density of 4.32 mA $cm^{-2}$ which found to be much superior to the TFBB-TAB based counterpart. The higher cathodic current density achieved with TFBB-TAT photocathode reflects its potentiality for water reduction under visible light illumination. Moreover, the cathodic current response of the TFBB-TAT electrode was found to be superior to TFBB-TAB throughout the studied cathodic potential region. The reversibility of the photoreactivity of the synthesized COF studied from the transient photocurrent response over several light on-off cycles. The transient photocurrent was recorded at a fixed potential of -0.5 V vs SCE. Figure 3b represents the transient photoresponse of the designed photocathodes. A sharp increase of negative current density was noticed on light illumination whereas the current response reverts back to the initial stage as the illumination shutdown. This rapid change of response current under dark and illumination state signifies good photoreversibility of the developed photocathodes. Moreover, the magnitude of transient photoresponse was found to be higher for TFBB-TAT as compared to the TFBB-TAB. The similar characteristics noticed in the polarization which reflects the better photoreactivity of the former over latter. The better photoreactivity of TFBB-TAT COF arises from its low band gap as compared to the TFBB-TAB counterpart. More importantly, the presence of triazine functionalities helps to improve the photoabsorption capacity in TFBB-TAT.[33] However; the TFBB-TAB counterpart does not have any such functionality for light harvesting. Thus, the photocurrect recorded in the TFBB-TAT electrode found to be enhanced as compared to the TFBB-TAB counterpart. The current response recorded with present photocathodes found to be comparable to many recently reported photocathodes.[34-36]

The efficiency of a photocathode for water reduction largely depends on its charge transfer characteristics at electrode/electrolyte interface. In order to study the charge transfer process at electrode/electrolyte interface we have executed impedance measurement. The complex impedance plot, known as Nyquist plot mostly used to understand the charge transport characteristics of an electrode/electrolyte interface. Figure 3c shows the Nyquist plots of designed photocathodes. The Nyquist plots of both electrodes consist of a semicircle arc in high frequency region followed by a straight line in the low frequency region. The diameter of the semicircle arc generally used to evaluate the charge transfer resistance ($R_{ct}$) of an electrode/electrolyte interface. A smaller diameter signifies lower charge transfer resistance and vice versa. Further, the low charge transfer resistance ascertains good charge transport from electrode to electrolyte which leads to a higher redox kinetics at the electrode surface. In present study the TFBB-TAT electrode exhibits lower $R_{ct}$ (17.12 Ω) than TFBB-TAB (21.74 Ω) electrode. This corroborates the higher charge transfer across TFBB-TAT/electrolyte interface as compared to the TFBB-TAB/electrolyte interface which results in a faster water reduction kinetics at the former electrode. Thus, the high photoresponse obtained with TFBB-TAB electrode attributed to its good photoabsorption capacity together with efficient charge transport characteristics. The long term photostability of designed photocathodes was insighted by executing ampreometric study under illuminated condition. The designed photocathode shows considerable retention of photocurrent density after 180 minutes of operation under visible light illumination (**figure 3**d). However, the

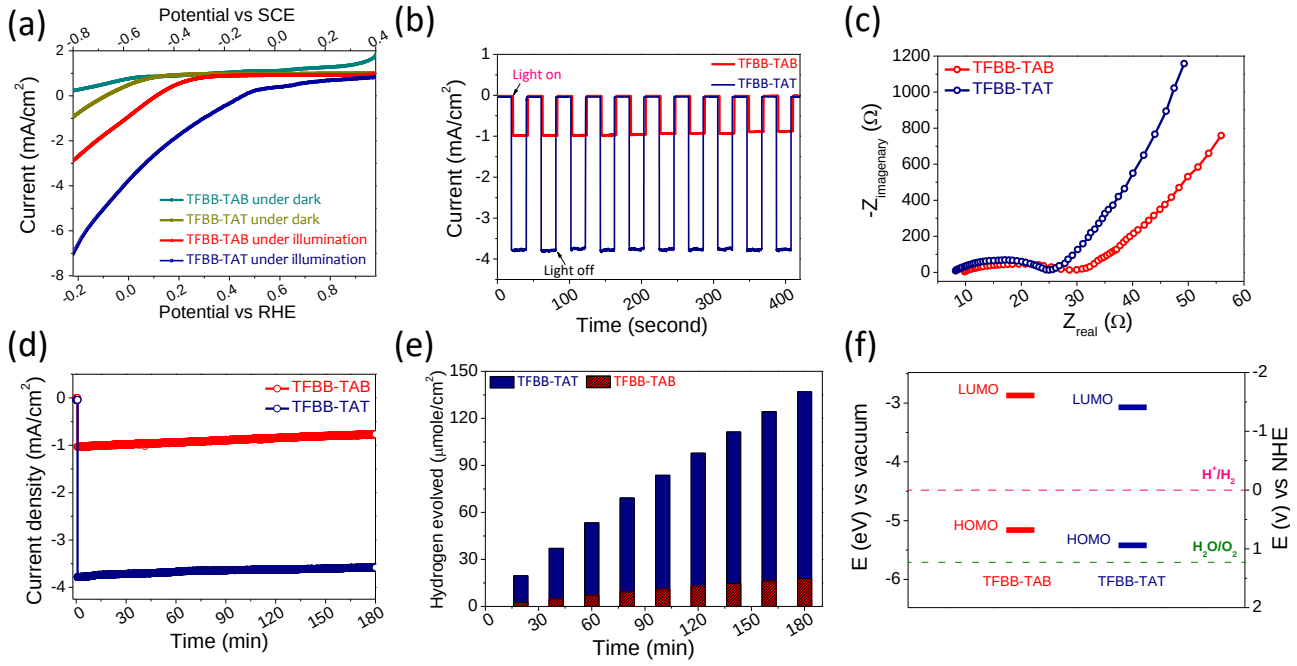


**Figure 3**: (a) Polarization plots of developed photocathodes under dark and illumination, (b) transient photo current response under dark and light (c) long term photostability of COF based photocathodes, (d) PEC hydrogen production profile of developed photocathodes, (f) band edge position of the developed TABB-TAT and TFBB-TAB COF.

TFBB-TAT photocathode (94 % retention) exhibits better stability than the TFS-TAB photocathode (73 % retention). The high stability of TFBB-TAT photocathode under illumination condition made it a potential candidate for efficient PEC water splitting application. The PEC water reduction capacity of developed photocathode was checked by measuring the quantity of hydrogen evolved during chronoamperiometric study at -0.5 V vs. SCE. Figure 3e shows the PEC hydrogen production profile of TFBB-TAT and TFBB-TAB based photocathdes. The TFBB-TAT photocathode offers a hydrogen production capacity of 137 µmol $cm^{-2}$ after 180 minute of PEC operation. Moreover, the hydrogen production capacity of TFBB-TAT electrode estimated to be 7.6 times higher than TFBB-TAB electrode. This superior hydrogen production activity of TFBB-TAT photocathode was attributed to its low band gap, higher photoabsorption capacity, and efficient charge transport capacity as compared to the TFBB-TAB photocathode. Further, the high surface area of present TFBB-TAT COF offers large number of active sites for water reduction on electrode surface. Previous reports on nitrogen reach COF for electrochemical water splitting (proton reduction) revels that –C=N- functionalities serves as active centre for proton reduction there by molecular hydrogen generation.[29] In present study both the synthesized COF has –C=N- functionalities on their structural unit which can serve as the active centre for water reduction. Thus, the number of –C=N- functionalities will determine the water reduction capacity of the COF modified photocathodes. In case of TFBB-TAT COF the number of –C=N- groups (six/structural unit) found to be two times higher than the TFBB-TAB (three/structural unit). The avaliabilty of higher number of electrocatalytic sites on the TFBB-TAT offers better water reduction capacity than TFBB-TAB COF. Moreover, the interconnected porous structure enhances the electrolyte diffusion on to the electrode surface resulting in faster electrode kinetics. The interlinked highly conjugated electronic structure of the synthesized COF helps achieve good electronic conductivity. The nitrogen rich TFBB-TAT electrode shows lower charge transfer resistance than TFBB-TAB counterpart. This may be attributed to the better electronic conductivity of former as compared to the latter. The performance of present TFBB-TAT photocathode was fond to be comparable to many previously reported photocathode for PEC water splitting (table S1).

## THEORETICAL AND MECHANISTIC CALCULATION:

To further prove the exact electron excitation and charge recombination, the band edge position for both the COFs were calculated (**figure 3**f).

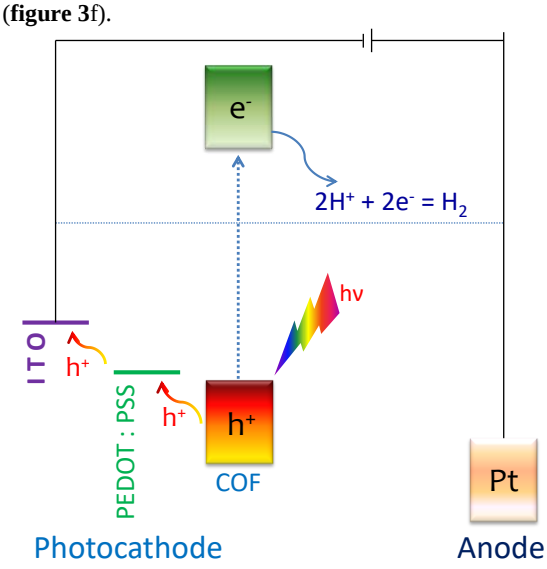


**Figure 4:** Schematic presentation for the possible electron transfer process.

The theoretical band gap for TFPB-TAT COF was determined by the DFT calculation which is 2.347 ev with the valence band energy of +0.91913 ev (*vs* NHE) and the conduction band energy of -1.428 eV (*vs* NHE). This band position shows that the driving force for the proton reduction is enough for the TFFB-TAT COF. However, the transfer of photogenerated hole becomes necessary to reduce the electron-hole pair recombination which helps to improve the effective utilization of photoexcited electrons for proton reduction. Thus, the presence of a proper hole transporting layer will improve the water reduction capacity of the designed photocathode. In present study PEDOT: PSS used as a hole transporting layer for hole transporting from COFs to ITO surface. The valance band maxima of PEDOT: PSS reported to be lies at 0.6 eV vs NHE (-5.0 eV vs vacuum) which can easily extract hole from the valance band of the synthesized COFs. Thus, the efficient charge separation in presence of hole transporting PEDOT: PSS layer offers a promising PEC performance. A schematic of chare transport mechanism of designed photcathode is depicted in Figure 4.

## CONCLUSION:

In conclusion, we present a new triazine based covalent organic framework which shows the superior water splitting with respect to the non-triazine counterpart through photoelectrochemical process. The triazine unit is found to be play an important role for the light harvesting and electrocatalytic water reduction. This enhance catalytic activity is due to the large surface area, satisfactory band gap and optimised planar structure for better electron charge separation. The photoelectrochemical HER performance of TFBB-TAT COF is comparable or even better in some cases than that of traditional metallic catalysts. The excellent stability and durability of TFBB-TAT COF as a photocathode in presence of light irradiation condition made it a potential candidate for in future efficient photoelectrochemical (PEC) hydrogen evolution reaction (HER) application. This finding should be of considerable interest to the materials chemistry as well as renewable energy community for next generation organic fuel cells.

## ASSOCIATED CONTENT

(Word Style "TE_Supporting_Information"). **Supporting Information**. A brief statement in nonsentence format listing the contents of material supplied as Supporting Information should be included, ending with "This material is available free of charge via the Internet at http://pubs.acs.org." For instructions on what should be included in the Supporting Information as well as how to prepare this material for publication, refer to the journal's Instructions for Authors.

## AUTHOR INFORMATION


### Corresponding Author

*E-mail for Dr. A.P.: msap5@iacs.res.in
*E-mail for Prof. S.B.: director@iacs.res.in


### Author Contributions

BCP, AP and SB designed the scheme. MA did the theoretical calculation. SK and DP executed the photoelectrochemical study.

### Notes

The authors declare no competing financial interest.

## ACKNOWLEDGMENT


AP & BCP acknowledge DST for funding through INSPIRE program. Prof. SB acknowledges support received from DST (J. C. Bose fellowship) and that from DRU at IACS.


## REFERENCES


(1) Mazloomi, K.; Gomes, C. Hydrogen as an energy carrier: Prospects and challenges. *Renew. Sust. Energ. Rev.***2012**, 16, 3024-3033.
(2) Turner, J. A. Sustainable hydrogen production. *Science* **2004**, 305, 972-974.
(3) Cabán-Acevedo, M.; Stone, M. L.; Schmidt, J.; Thomas, J. G.; Ding. Q; Chang, H. C.; Tsai, M. L; He, J. H.; Jin, S. Efficient hydrogen evolution catalysis using ternary pyrite-type cobalt phosphosulphide.*Nat. Mater.***2015**, 14, 1245-1251.
(4) Christopher, K.; Dimitrios, R. A review on exergy comparison of hydrogen production methods from renewable energy sources. *Energy Environ. Sci*. **2012**, 5, 6640.
(5) Heller, A.; Conversion of Sunlight into Electrical Power and Photoassisted Electrolysis of Water in Photoelectrochemical Cells. *Acc. Chem. Res.***1981**, 14, 154-162.
(6) May, M. M.; Lewerenz, H. J.; Lackner, D.; Dimroth, F.; Hannappel, T. Efficient direct solar-to-hydrogen conversion by in situ interface transformation of a tandem structure. *Nat. Commun.***2015**, 6, 8286.
(7) Lewis, N. S.; Nocera, D. G. Powering the planet: Chemical challenges in solar energy utilization. *Proc. Natl. Acad. Sci. U.S.A.***2006**, 103, 15729.
(8) Landman, A.; Dotan, H.; Shter, G. E.; Wullenkord, M.; Houaijia, A.; Maljusch, A.; Grader, G. S.; Rothschild, A. Photoelectrochemical water splitting in separate oxygen and hydrogen cells. *Nat. Mater.***2017**, 16, 646-651.
(9)Tee, S. Y.; Win, K. Y.; Teo, W. S.; Koh, L. D.; Liu, S.; Teng, C. P.; Han, M. Y. Recent Progress in Energy-Driven Water Splitting. *Adv.Sci.***2017**, 4, 1600337.
(10) Kudo, A.; Miseki, Y.; Heterogeneous photocatalyst materials for water splitting. *Chem. Soc. Rev.***2009**, 38, 253-278.
(11) Khaselev, O.; Turner, J. A.; A Monolithic Photovoltaic-Photoelectrochemical Device for Hydrogen Production via Water Splitting.*Science***1998**, 280, 425-427.
(12) Subbaraman R.; Tripkovic D.; Strmcnik D.; Chang K. C.; Uchimura M.; Paulikas A. P.; Stamenkovic V.; Markovic N. M. Enhancing Hydrogen Evolution Activity in Water Splitting by Tailoring $Li^+$-$Ni(OH)_2$-Pt Interfaces, *Science***2011**, 334, 1256-1260.
(13) McCrory, C. C. L.; Jung, S.; Ferrer, I. M.; Chatman, S. M.; Peters, J. C.; Jaramillo. T. F. Benchmarking Hydrogen Evolving Reaction and Oxygen Evolving Reaction Electrocatalysts for Solar Water Splitting Devices. *J. Am. Chem. Soc.***2015**, 137, 4347-4357.
(14) Laursen, A. B.; Kegnæs, S.; Dahl, S.; Chorkendorff, I. Molybdenum sulphides-efficient and viable materials for electro and photoelectrocatalytic hydrogen evolution. *Energy Environ. Sci.***2012**, 5, 5577-5591.
(15) Wang, W.; Xu, X.; Zhou, W.; Shao, Z. Recent Progress in Metal Organic Frameworks for Applications in Electrocatalytic and Photocatalytic Water Splitting. *Adv. Sci*. **2017**, 4, 1600371.
(16) Li, J.; Yan, M.; Zhou, X.; Huang, Z.Q.; Xia, Z.; Chang, C. R.; Ma, Y.; Qu, Y. Mechanistic Insights on Ternary $Ni_{2-x}Co_xP$ for Hydrogen Evolution and their Hybrids with Graphene as Highly Efficient and Robust Catalysts for Overall Water Splitting. *Adv. Funct. Mater.***2016**, 26, 6785-6796.
(17) Côté, A. P.; Benin, A. I.; Ockwig, N. W.; O'Keeffe, M.; Matzger, A. J.;Yaghi.O. M. Porous, crystalline, covalent organic frameworks. *Science***2005**, 310, 1166-1170.
(18) Romo, F. J. U.; Hunt, J. R.; Furukawa, H.; Klöck, C.; O'Keeffe, M.; Yaghi, O. M. A Crystalline Imine-Linked 3-D Porous Covalent Organic Framework. *J. Am. Chem. Soc.***2009**, 131, 4570-4571.
(19) Kandambeth, S.; Mallick, A.; Lukose, B.; Mane, M. V.; Heine, T.; Banerjee, R. Construction of Crystalline 2D Covalent Organic Frameworks with Remarkable Chemical (Acid/Base) Stability via a Combined Reversible and Irreversible Route. *J. Am. Chem. Soc.***2012**, 134, 19524-19527.
(20) Huang, N.; Wang, P.; Jiang, D. Covalent organic frameworks: a materials platform for structural and functional designs, *Nat. Rev. Mater.***2016**, 1, 16068.
(21) Medina, D. D.; Sick, T.; Bein, T. Photoactive and Conducting Covalent Organic Frameworks, *Adv. Energy Mater*.**2017**, 7, 1700387.

(22) Feng, X.; Liu, L.; Honsho, Y.; Saeki, A.; Seki, S.; Irle, S.; Dong, Y.; Nagai, A.; Jiang, D. High-Rate Charge-Carrier Transport in Porphyrin Covalent Organic Frameworks: Switching from Hole to Electron to Ambipolar Conduction. *Angew. Chem. Int. Ed.***2012**, 51, 2618-2622.
(23) Dogru, M.; Handloser, M.; Auras, F.; Kunz, T.; Medina, D.; Hartschuh, A.; Knochel, P.; Bein, T. A Photoconductive Thienothiophene-Based Covalent Organic Framework Showing Charge Transfer Towards Included Fullerene. *Angew. Chem. Int. Ed.***2013**, 52, 2920-2924.
(24) Xie, J.; Shevlin, S. A.; Ruan, Q.; Moniz, S. J. A.; Liu, Y.; Liu, X.; Li, Y.; Lau, C. C.; Guo, Z. X.; Tang, J. Efficient visible light-driven water oxidation and proton reduction by an ordered covalent triazine-based framework. DOI: 10.1039/C7EE02981K.
(25) Sick, T.; Hufnage, A. G.; Kampmann, J.; Kondofersky, I.; Calik, M.; Rotter, J. M.; Evans,A.; Döblinger, M.; Herbert, S.; Peters, K.; Böhm, D.; Knochel, P.; Medina, D. D.; Rohlfing, D. F.; Bein, T. Oriented Films of Conjugated 2D Covalent Organic Frameworks as Photocathodes for Water Splitting. *J. Am. Chem. Soc.***2018**, 140, 2085-2092.
(26) Patra, B. C.; Khilari, S.; Manna, R. N.; Mondal, S.; Pradhan, D.; Pradhan, A.; Bhaumik, A. A Metal-Free Covalent Organic Polymer for Electrocatalytic Hydrogen Evolution. *ACS Catal.* **2017**, 7, 6120-6127.
(27) Bhunia, S.; Das, S. K.; Jana, R.; Peter, S. C.; Bhattacharya, S.; Addicoat, M.; Bhaumik, A.; Pradhan. A. Electrochemical Stimuli-Driven Facile Metal-Free Hydrogen Evolution from Pyrene-Porphyrin-Based Crystalline Covalent Organic Framework. *ACS Appl. Mater. Interfaces*, **2017**, 9, 23843-23851.
(28) Stegbauer, L.; Schwinghammer, K.; Lotsch, B. V.A hydrazone-based covalent organic framework for photocatalytic hydrogen production. *Chem. Sci.***2014**, 5, 2789-2793.
(29) Vyas, V. S.; Haase, F.; Stegbauer, L.; Savasci, G.; Podjaski, F.; Ochsenfeld, C.; Lotsch, B. V. A tunableazine covalent organic framework platform for visible light-induced hydrogen generation, *Nat. Commun.* **2015**, 6, 8508.
(30) Jiang, X.; Wanga,; P. Zhao, J. 2D covalent triazine framework: a new class of organic photocatalyst for water splitting, *J. Mater. Chem. A* **2015**, 3, 7750-7758.
(31) May, M. M.; Lewerenz, H. J.; Lackner, D.; Dimroth, F.; Hannappel, T. Efficient direct solar-to-hydrogen conversion by in situ interface transformation of a tandem structure. *Nat. Commun.***2015**, 6, 8286.
(32) Morales-Guio, C.G.; Tilley, S. D.; Vrubel, H.; Grätzel, M; Hu, X.. Hydrogen evolution from a copper (I) oxide photocathode coated with an amorphous molybdenum sulphide catalyst. *Nat. Commun.* **2014**, 5, 3059.
(33) Zheng, Y.; Jiao, Y.; Zhu, Y.; Li, L. H.; Han, Y.; Chen, Y.; Du, A.; Jaroniec, M.; Qiao, S. Z. Hydrogen evolution by a metal-free electrocatalyst. *Nat. Commun.* **2014**, 5, 3783.
(34) Chen, C. J.; Chen, P. T.; Basu, M.; Yang, K. C.; Lu, Y. R.; Dong, C. L.; Ma, C. G.; Shen, C. C.; Hu, S. F.; Liu, R. S. An integrated cobalt disulfide (CoS2) co-catalyst passivation layer on silicon microwires for photoelectrochemical hydrogen evolution. *J. Mater. Chem. A* **2015**, 3, 23466-23476.
(35) Downes, C. A.; Marinescu. S. C. Efficient Electrochemical and Photoelectrochemical $H_2$ Production from Water by a Cobalt Dithiolene One-Dimensional Metal-Organic Surface. *J. Am. Chem. Soc.* **2015**, 137, 13740-13743.
(36) Meng, P.; Wang, M.; Yang, Y.; Zhang, S.; Sun, L. CdSe quantum dots/molecular cobalt catalyst co-grafted open porous NiO film as a photocathode for visible light driven $H_2$ evolution from neutral water. *J. Mater. Chem. A* **2015**, 3, 18852-18859.
.
.